Review of Scientific Instruments

Design of multi neutron-to-gamma converter array for measuring time resolved ion temperature of inertial confinement fusion implosions

Cite as: Rev. Sci. Instrum. **93**, 083520 (2022); https://doi.org/10.1063/5.0101887
Submitted: 03 June 2022 • Accepted: 04 August 2022 • Published Online: 30 August 2022

K. D. Meaney, Y. Kim, N. M. Hoffman, et al.

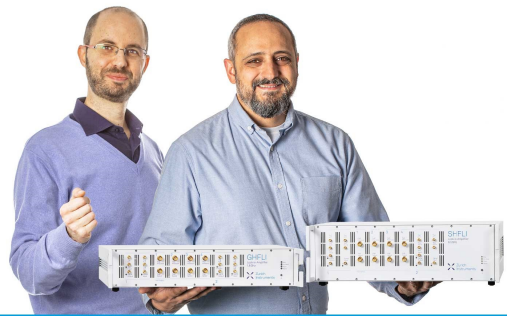

Review of Scientific Instruments ARTICLE scitation.org/journal/rsi

Design of multi neutron-to-gamma converter array for measuring time resolved ion temperature of inertial confinement fusion implosions

Cite as: Rev. Sci. Instrum. 93, 083520 (2022); doi: 10.1063/5.0101887
Submitted: 3 June 2022 • Accepted: 4 August 2022 •
Published Online: 30 August 2022

K. D. Meaney,[1,a)] Y. Kim,[1] N. M. Hoffman,[1] H. Geppert-Kleinrath,[1] J. Jorgenson,[1] M. Hochanadel,[1] B. Appelbe,[2] A. Crilly,[2] R. Basu,[2] E. Y. Saw,[2] A. Moore,[3] and D. Schlossberg[3]

AFFILIATIONS

[1] Los Alamos National Laboratory, Los Alamos, New Mexico 87545, USA
[2] Centre for Inertial Fusion Studies, Imperial College London, London, United Kingdom
[3] Lawrence Livermore National Laboratory, Livermore, California 94550, USA

Note: This paper is part of the Special Topic on Proceedings of the 24th Topical Conference on High-Temperature Plasma Diagnostics.
[a)] **Author to whom correspondence should be addressed:** meaney@lanl.gov

ABSTRACT

The ion temperature varying during inertial confinement fusion implosions changes the amount of Doppler broadening of the fusion products, creating subtle changes in the fusion neutron pulse as it moves away from the implosion. A diagnostic design to try to measure these subtle effects is introduced—leveraging the fast time resolution of gas Cherenkov detectors along with a multi-puck array that converts a small amount of the neutron pulse into gamma-rays, one can measure multiple snapshots of the neutron pulse at intermediate distances. Precise measurements of the propagating neutron pulse, specifically the variation in the peak location and the skew, could be used to infer time-evolved ion temperature evolved during peak compression.

I. INTRODUCTION

In inertial confinement fusion (ICF), a small capsule is compressed with high-powered lasers to high temperatures and densities and undergoes nuclear fusion.[1] While fusion performance of implosions has steadily improved over the years,[2] a milestone has been achieved at the National Ignition Facility (NIF) that has created a burning plasma[3] with higher yields and a new physics regime.

To understand the fusion hot spot physics and improve performance, a primary goal is to diagnose implosions to quantify the as-shot performance, energy budget, and dynamics of the formed hot spot—especially in the near ignition regime. In ICF, the fusion process is highly sensitive to the ion temperature, as the deuterium–tritium (DT) fusion rate is proportional to the third or fourth power at keV temperatures.[4] Furthermore, the processes that affect the ion temperature—alpha particle deposition, radiation, and conduction transfer—evolve quickly compared to the hydrodynamic evolution of the imploding capsule. Measuring how the ion temperature evolves near peak implosion is closely connected to the performance and energy balance of the implosion.[5,6] A poor-performing capsule sees a negative ion temperature slope as the hot spot cools even before peak implosion,[7] an igniting capsule continues adding heat from the fusion process with a sharply positive ion temperature slope until the capsule blowing apart decreases the density enough to stop the fusion burn. The value of the slope of the ion temperature can probe the energetic race between the capsule's evolution and the DT fusion depositing energy. The Lawson criteria can be written in the form of the concavity of the ion temperature.[8]

Although the burn-averaged ion temperature is routinely measured using neutron time of flight techniques,[9,10] a time-resolved ion temperature is currently not measured. Techniques have been suggested, such as a time-resolved magnetic recoil spectrometer

[MRS(t)], which development continues[11] and extremely fast reaction history measurements.[6] Here, we propose an alternative technique to utilize a differential fusion gamma ray and neutron measurement[12] to attempt to measure the time dependence of the neutron Doppler broadening in order to infer the time-resolved ion temperature. This technique leverages Cherenkov gamma-ray detectors,[13] specifically for their high temporal resolution.

When DT fusion occurs, the created neutrons contain information about the temperature through the Doppler broadening of their energy spectrum. The fusion evolves over the reaction history, $Y_n(t)$, and the ion temperature also evolves, $\theta(t)$; therefore, the Doppler broadening of the released neutrons also varies. A highly precise measurement, M_{DTn}, of the neutron pulse at some distance is a convolution of the reaction history, the neutron arrival history to distance d, which depends on the time-dependent ion temperature, $N(t, d, \theta(t))$, the effect from a neutron-to-gamma ray converter material, $\Delta_{n,\gamma}$, henceforth called a puck, and a gamma-ray detector instrument response, $I(t)$,

$$M_{DTn}(t) = Y_n(t) \otimes N(t, d, \theta(t)) \otimes \Delta_{n,\gamma} \otimes I(t). \quad (1)$$

Using the DT fusion gamma rays to directly measure the reaction history with the same instrument gives the convolution

$$M_{DT\gamma}(t) = Y_n(t) \otimes I(t). \quad (2)$$

In theory, with both of these measurements and knowledge of $\Delta_{n,\gamma}$, a forward fitting procedure can follow the convolution to solve for the time-dependent ion temperature. In reality, the time dependence of the ion temperature has a minor, subtle effect that is neglected with neutron time of flight diagnostics. Conceptually, the challenge is to measure the effect of neutrons being created early having less Doppler broadening compared to neutrons created later having more Doppler broadening, for example, an increasing temperature. To make such a measurement feasible, the neutron pulse must be measured with extremely high temporal resolution and low noise.

We propose to make both reaction history, $M_{DT\gamma}$, and multiple neutron pulse measurements, M_{DTn}, using a gas Cherenkov detector (GCD) fitted with a multi-puck structure that converts a small percentage of the propagating neutrons into a gamma ray signal that can also be measured at multiple, intermediate distances with high time resolution, a cartoon of the layout is shown in Fig. 1. A measurement with high enough fidelity will be able to infer the time dependent ion temperature.

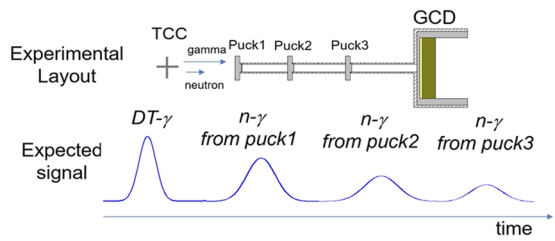

FIG. 1. An illustrative cartoon of the multi-puck array design and expected signals. The front of a gas Cherenkov detector is fixed with a structure that holds multiple pucks. As an implosion releases gamma rays and neutrons, the detector first records the DT fusion gamma signal as they move at the speed of light to the detector. The neutrons then follow, with a small amount scattering with the puck, which, through an $(n, n')\gamma$ interaction, release a gamma ray pulse. Multiple neutron pulse measurements can constrain the time-dependent ion temperature.

II. MODEL, ASSUMPTIONS AND EFFECT OF $T_{ion}(t)$

A neutron energy spectrum due to a Maxwellian ion temperature has the form[14]

$$f(E)dE = dE \times \exp\left(-(E_n - \langle E_n \rangle)^2 \Big/ \left(\frac{4m_n\theta\langle E_n\rangle}{m_n + m_\alpha}\right)\right), \quad (3)$$

where $\langle E_n \rangle$ = 14.05 MeV is the average energy of the emitted DT fusion neutron, m_n is the mass of the neutron, m_α is the mass of the alpha particle, and θ is the thermal temperature of the plasma. An instantaneous pulse released at t_1 with a temperature, θ, measured with a detector at a distance, d, will have a neutron pulse in the shape[15]

$$N(t, d, \theta) = Ae^{-\frac{(t-(t_n+t_1))^2}{2\sigma_\theta^2}}, \quad (4)$$

where A is a normalization constant, $t_n = d \times \sqrt{\frac{m_n}{2\langle E_n\rangle}}$ is the 14.05 MeV neutron arrival time, and $\sigma_\theta = \frac{m_n d}{2\sqrt{m_n+m_\alpha}E_n}\sqrt{\theta}$. An extended reaction history can be broken into a continuum of instantaneous broadening pulses. A neutron pulse broadening as it propagates away from the implosion can be calculated through an integral over the product of the reaction history and the temporal broadening. For example, the neutron pulse from a Gaussian fusion reaction history with bang time at t_{BT} and width σ_{DT} takes the form

$$N(t, d) = \int_{-\infty}^{\infty} \left(Ae^{-\frac{(t_i-t_{BT})^2}{2\sigma_{DT}^2}}\right) \times e^{-\frac{(t-(t_n+t_i))^2}{2\sigma_\theta^2}} dt_i$$
$$= Ae^{-\frac{(t-(t_{BT}+t_n))^2}{2(\sigma_{BT}^2+\sigma_\theta^2)}}. \quad (5)$$

Now consider, instead of a constant temperature, a temperature that changes linearly in the form $\sigma_\theta^2 = \frac{m_n^2 d^2}{4(m_n+m_\alpha)E_n^2}\dot{\theta}t_i = c \times t_i$. The neutron pulse can then be calculated in the form

$$N(t, d) = \int_0^{\infty} \left(Ae^{-\frac{(t_i-t_{BT})^2}{2\sigma_{DT}^2}}\right) \times e^{-\frac{(t-(t_n+t_i))^2}{2c*t_i}} dt_i. \quad (6)$$

To our knowledge, the integral has no analytic solution but can be completed numerically. The idealized example considered here shows a distinctive relationship between skew and time-varying ion temperature for the case of a Gaussian burn history and linear temperature profiles. Work is ongoing to fully quantify this relationship such that a measure of the time-varying ion temperature can be calculated in more complex scenarios, the details of which will be published elsewhere.[16]

A simplified numerical model has been developed to calculate the effects of the ion temperature–time evolution. Taking the inputs of a reaction history, a time-dependent ion temperature and a detector distance, at each time step (1 ps), a Gaussian neutron pulse is calculated with the width from Eq. (4) from the temperature at that time and the amplitude from the reaction history at that time. Each time step creates a neutron pulse, which is then all added together for the net neutron pulse at that distance. Note that this model does

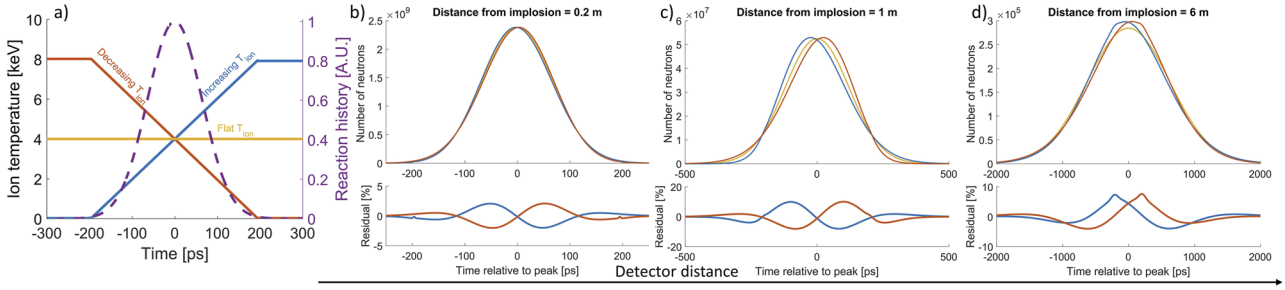

FIG. 2. Output from the neutron broadening model. The left figure shows the calculated idealized Gaussian reaction history (dashed purple curve) and three temporal profiles of ion temperature, a linearly increasing case (blue solid line), a linearly decreasing case (red solid line), and a flat case (yellow solid line). All three of these cases have a burn-averaged value of 4 keV. The calculated neutron pulse at 0.2, 1, and 6 m distances are shown for each case. The residual plot beneath each peak shows the difference between the evolving T_{ion} cases and the flat case. The effect of the evolving ion temperature has a minor effect, causing a residual on the order of a few percent.

not include effects from signal to noise, downscattered neutrons, internal flows, relativistic effects, and assumes a Maxwellian temperature with both deuterium and tritium at the same temperature. Moore *et al.* has a parallel model and studied the effect of noise[17] and concluded that signal-to-noise ratios of 1%–2% are needed to observe the skew at high enough precision. In addition, Schlossberg *et al.* completed a study using neutron time of flight at intermediate distances with an analog Monte Carlo reconstruction model.[18]

An idealized example, which takes a Gaussian reaction history with a 150 ps burnwidth [full width half max (FWHM)], a yield of 10^{14} DT fusions, an average ion temperature, kT, of 4 keV, and a constant slope across the fusion burn of $\pm 20 \frac{\text{keV}}{\text{ns}}$ or $\pm 3 \frac{\text{keV}}{150\ \text{ps}}$, is used to get an approximate estimate for the detector system. This nominal condition was estimated as reasonable values for a range of simulated OMEGA-like capsules. Figure 2 shows some selected outputs from the numerical model, showing a comparison against a constant ion temperature or an ion temperature that evolves through the burn.

To further characterize the neutron pulse, the following metrics are taken of each neutron pulse output: (1) peak maximum, (2) peak centroid, mean, or first moment, defined as $\mu = \frac{1}{t_{end}-t_1}\int_{t_1}^{t_{end}} t \times N(t)dt$, (3) FWHM—proportional to second moment as $\sigma \approx FWHM(N(t))/2.355$, (4) skew, the normalized third moment about the mean, defined as skew $= \frac{1}{\sigma^3}\frac{1}{t_{end}-t_1}\int_{t_1}^{t_{end}}(t-\mu)^3 N(t)dt$ and (5) the kurtosis, or the normalized fourth moment about the mean, defined as kurt $= \frac{1}{\sigma^4}\frac{1}{t_{end}-t_1}\int_{t_1}^{t_{end}}(t-\mu)^4 N(t)dt$. Note that the peak maximum is a convolution of the peak centroid and skew, but the diagnostic distinguishability of the peak maximum is different than taking the moments, and so it is included for comparison. These characterizations as a function of detector distance for the two implosion types presented are shown in Fig. 3. The results show that the centroid relative to t_n, width, and kurtosis likely do not have a diagnostically measurable signature because measuring single picosecond variation differences is difficult. The strongest signal relies on the peak maximum location, on the order of 10 s of ps from the expected mean neutron energy time of arrival and the skew, which is on the order of a few percent. The model also shows that intermediate regions, a few meters, are where the effect of the ion temperature slope is most prominent, in agreement with Moore *et al.*[17]

III. PROPAGATION OF SIGNAL IN A MULTI-PUCK DESIGN

In the multi-puck design, the GCD3[19] detector will have pucks connected to it that create a gamma-ray pulse as the neutron pulse scatters with it. The neutron pulse interacts with each puck and creates a gamma-ray signal that is measured by the GCD. The GCD3 can be put at its highest operating pressure to measure all gamma-rays above 1.8 MeV for its highest signal level. The 14 MeV neutron to gamma-ray cross section can be evaluated with the nuclear databases as calculated with Monte Carlo n-particle software (MCNP).[20] Carbon has the highest >1.8 MeV neutron to gamma-ray efficiency (6.3×10^{-2} Cherenkov photons/fusion) combined with a graphite density of 2.1 $\frac{\text{g}}{\text{cm}^3}$ due to its bright 4.4 MeV line.[21] Other reasonable materials, such as aluminum (3.3×10^{-2} Cherenkov photons/fusion, 2.3 $\frac{\text{g}}{\text{cm}^3}$) and tungsten ($4.5 \times 10^{-3}$ Cherenkov photons/fusion, 19.2 $\frac{\text{g}}{\text{cm}^3}$), have lower neutron to gamma ray

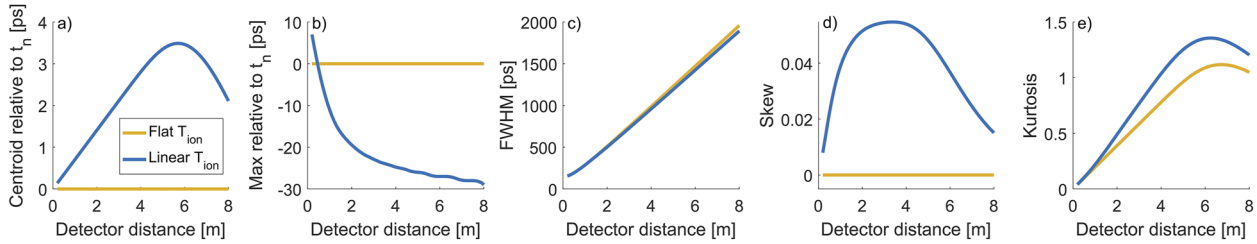

FIG. 3. Outputs of the moments and maximum of the neutron pulses as a function of detector distance. Likely, only the peak max and skew are the only diagnostically measurable signals. The effect of the skew has an optimum at an intermediate distance of around 2–5 m.

conversion. For a graphite puck of 0.3 cm thickness, it is expected to attenuate only 2.5% of a 4.4 MeV gamma-ray signal.

The detector should use at least three pucks. Doing a moment analysis of the neutron time of flight requires at least four neutron pulse measurements, including the reaction history measurement, at different locations in order to exactly solve the deconvolution in Eq. (2), the details of which will be shown elsewhere.[16] Furthermore, having multiple measurements allows for a relative comparison between the two measurements instead of an absolute measurement. Additional measurements will give more constraints in a forward model or deconvolution.

The geometry of the puck system induces a puck instrument response function depending on the different times of transit from neutrons arriving at the puck and gamma-rays arriving at the front face of the GCD. There is an impulse broadening from the difference in transit time from the neutron/gamma-ray from the top of the puck compared to the middle of the puck. This effect is minimized by placing the puck further from the implosion and the face of the GCD. The signal is also broadened by the thickness of the puck due to the neutron time of transit across the puck, for example, a 0.3 cm thick puck introduces a 58 ps broadening. Decreasing the thickness linearly decreases the signal. MCNP was used to calculated the effects of geometry on the puck response[20] for the above 1 m example as well as the fielded prototype puck fielded at 14 cm, discussed below. The output showed an FWHM response of 90–103 ps but also an induced skew of value 0.25–0.35 from the particle arrival times. A parabolic puck shape can be used to minimize particle transit times. When the gamma-ray signals are measured, the temporal instrumental response of a GCD is dominated by the Photek 110 photomultiplier tube (PMT),[22] a ringing response with an FWHM of around 110 ps, although the peak co-timing is around 7 ps.[7] A simple convolution study confirms that a neutron pulse's skew is well maintained through the convolution of the PMT response, neglecting the effects of noise. Therefore, taking the skew of the measured signal, without applying a deconvolution or forward fit, will maintain the induced skew of the signal above the inherent skew in the instrument response function (IRF).

Both the puck-induced instrument response and the GCD instrument response induce inherent skews and broadening in any measured signal. With precise enough knowledge of both, through geometric modeling of the puck and instrument measurements, their effects can be known well enough to remove their influence. The diagnostic challenge is measuring the induced skew from the $T_{ion}(t)$ on top of the uncertainty from these effects. This can be achieved by measuring longer signals (pucks at further distances), increasing the signal-to-noise ratios, and better calibration of these instrument responses.

IV. FIELDING OF MECHANICAL PROTOTYPE

A prototype of a puck system, made to test GCD mating and mechanical properties, has been fielded at the OMEGA facility with a single puck at a distance of 14 cm from an ICF implosion. A computer-aided design (CAD) model is shown in Fig. 4. At this short distance, the amount of broadening, as estimated by Eq. (4), is 5 ps, too short for any noticeable effect from the ion temperature or skew. The GCD was set to a 6.3 MeV energy threshold with an aluminum puck 6 cm from the converter of the GCD with a Photek 110 set to

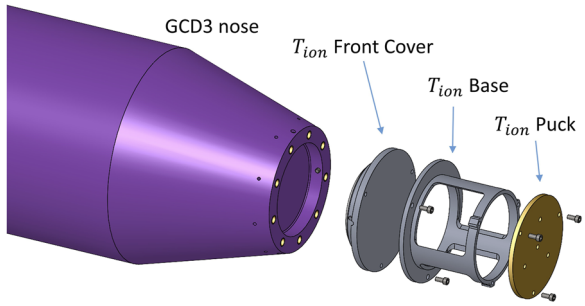

FIG. 4. CAD model of the prototype single puck model fielded at the OMEGA facility. The puck is 8.5 cm from the front of the GCD3, and the front of the puck was placed 14 cm from the implosion.

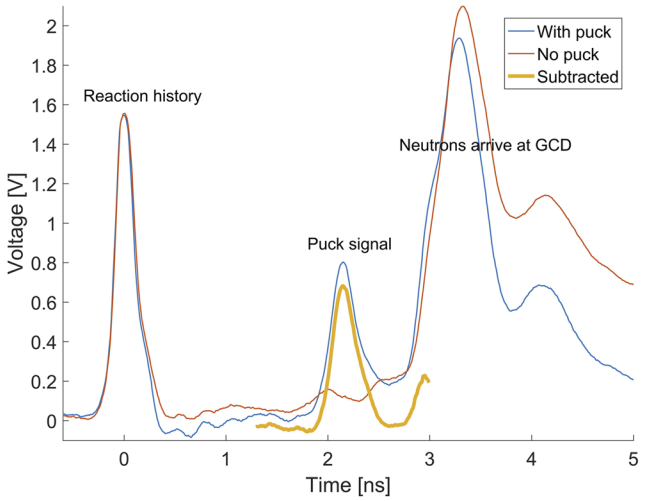

FIG. 5. The data collected from the prototype single puck system with two shots, one with the puck structure and one without. The isolated signal is from the subtraction of the two. The slight skew observed on the puck signal is consistent with the estimated geometric puck response function at that distance.

a quantum efficiency and gain net amplification of 6.7×10^4, corresponding to 4×10^3 photons collected on the GCD PMT, giving a statistic variance of 1.6%. The data are shown in Fig. 5. Taking the subtracted baseline noise root mean square, the background level is 5%. This background, according to Moore *et al.*,[17] is too large to successfully differentiate the skew if a physics measurement was made. Future designs will collect more photons through a lower Cherenkov gas threshold, and using carbon as a material instead of aluminum will bring the statistics below 1%. Furthermore, using a higher bit scope to reduce bit noise, collecting a more optimized voltage and, most importantly, having less non-puck supporting material and placing pucks further away from other material and diagnostics to reduce other potential scatter sources will reduce the subtraction between the puck and no puck conditions. With these improvements, if the signal-to-noise ratio can be improved by a factor or 2× or 4× it is likely the skew measurement can be made with confidence.

V. CONCLUSION

The time-resolved ion temperature may potentially be measured through precise measurement of the neutron pulse and

reaction history. Through the use of a multi-puck structure connected to the nose of a GCD, the fast time resolution of the gamma-ray detector may be leveraged to make a successful measurement. A simple model suggests that the diagnostic signature of the time-dependent ion temperature is an induced skew of the order of a few percent change and a peak timing shift of a few 10 s of ps. Understanding the induced puck and gamma-ray instrument response is important for the interpretation of the data.

Looking forward, a multi-puck design using carbon pucks with a parabolic shape, a minimal puck supporting structure with three to four pucks placed at an intermediate distance of 1–2 m, may give the best chance for a clean measurement.

ACKNOWLEDGMENTS

This research was supported by the Laboratory Directed Research and Development Program of Los Alamos National Laboratory under Project No. 20220294 ER.

AUTHOR DECLARATIONS

Conflict of Interest

The authors have no conflicts to disclose.

Author Contributions

K. D. Meaney: Conceptualization (equal); Data curation (equal); Formal analysis (equal); Funding acquisition (equal); Investigation (equal); Project administration (equal); Supervision (equal); Writing – original draft (equal); Writing – review & editing (equal). **Y. Kim**: Conceptualization (equal); Funding acquisition (equal); Investigation (equal); Project administration (supporting). **N. M. Hoffman**: Conceptualization (equal); Data curation (equal); Formal analysis (equal); Methodology (equal); Writing – review & editing (equal). **H. Geppert-Kleinrath**: Data curation (equal); Formal analysis (equal); Investigation (equal). **J. Jorgenson**: Formal analysis (supporting); Investigation (supporting). **M. Hochanadel**: Formal analysis (supporting); Investigation (supporting). **B. Appelbe**: Conceptualization (supporting); Investigation (supporting). **A. Crilly**: Conceptualization (supporting); Investigation (supporting). **R. Basu**: Conceptualization (supporting); Investigation (supporting). **E. Y. Saw**: Conceptualization (supporting); Investigation (supporting). **A. Moore**: Formal analysis (equal). **D. Schlossberg**: Formal analysis (supporting).

DATA AVAILABILITY

The data that support the findings of this study are available from the corresponding author upon reasonable request.

REFERENCES

[1] E. I. Moses, J. D. Lindl, M. L. Spaeth, R. W. Patterson, R. H. Sawicki, L. J. Atherton, P. A. Baisden, L. J. Lagin, D. W. Larson, B. J. MacGowan, G. H. Miller, D. C. Rardin, V. S. Roberts, B. M. V. Wonterghem, and P. J. Wegner, Fusion Sci. Technol. **69**, 1–24 (2016).

[2] O. A. Hurricane, D. A. Callahan, P. T. Springer, M. J. Edwards, P. Patel, K. Baker, D. T. Casey, L. Divol, T. Döppner, D. E. Hinkel, L. F. Berzak Hopkins, A. Kritcher, S. Le Pape, S. Maclaren, L. Masse, A. Pak, L. Pickworth, J. Ralph, C. Thomas, A. Yi, and A. Zylstra, "Beyond alpha-heating: Driving inertially confined fusion implosions toward a burning-plasma state on the National Ignition Facility," Plasma Phys. Controlled Fusion **61**, 014033 (2018).

[3] A. B. Zylstra, O. A. Hurricane, D. A. Callahan *et al.*, Nature **601**, 542–548 (2022).

[4] J. R. Langenbrunner and J. M. Booker, "Power index tables for burning D-T and D-D plasma," Los Alamos Technical Reports, LA-UR-18-22364, March, 2018.

[5] J. A. Frenje, T. J. Hilsabeck, C. W. Wink, P. Bell, R. Bionta, C. Cerjan, M. Gatu Johnson, J. D. Kilkenny, C. K. Li, F. H. Séguin, and R. D. Petrasso, Rev. Sci. Instrum. **87**, 11D806 (2016).

[6] Y. Arikawa, M. Ota, M. Nakajima, T. Shimizu, S. Segawa, T. N. Khoa Phan, Y. Sakawa, Y. Abe, A. Morace, S. R. Mirfayzi, A. Yogo, S. Fujioka, M. Nakai, H. Shiraga, H. Azechi, R. Kodama, K. Kan, J. Frenje, M. Gatu Johnson, A. Bose, N. V. Kabadi, G. D. Sutcliffe, P. Adrian, C. Li, F. H. Séguin, and R. Petrasso, Rev. Sci. Instrum. **91**, 063304 (2020).

[7] K. D. Meaney, N. M. Hoffman, Y. Kim, H. Geppert-Kleinrath, H. W. Herrmann, C. Cerjan, O. L. Landen, and B. Appelbe, Phys. Plasmas **28**, 032701 (2021).

[8] P. K. Patel, P. T. Springer, C. R. Weber, L. C. Jarrott, O. A. Hurricane, B. Bachmann, K. L. Baker, L. F. Berzak Hopkins, D. A. Callahan, D. T. Casey, C. J. Cerjan, D. S. Clark, E. L. Dewald, L. Divol, T. Döppner, J. E. Field, D. Fittinghoff, J. Gaffney, V. Geppert-Kleinrath, G. P. Grim, E. P. Hartouni, R. Hatarik, D. E. Hinkel, M. Hohenberger, K. Humbird, N. Izumi, O. S. Jones, S. F. Khan, A. L. Kritcher, M. Kruse, O. L. Landen, S. Le Pape, T. Ma, S. A. MacLaren, A. G. MacPhee, L. P. Masse, N. B. Meezan, J. L. Milovich, R. Nora, A. Pak, J. L. Peterson, J. Ralph, H. F. Robey, J. D. Salmonson, V. A. Smalyuk, B. K. Spears, C. A. Thomas, P. L. Volegov, A. Zylstra, and M. J. Edwards, Phys. Plasmas **27**, 050901 (2020).

[9] V. Y. Glebov, T. C. Sangster, C. Stoeckl, J. P. Knauer, W. Theobald, K. L. Marshall, M. J. Shoup, T. Buczek, M. Cruz, T. Duffy, M. Romanofsky, M. Fox, A. Pruyne, M. J. Moran, R. A. Lerche, J. McNaney, J. D. Kilkenny, M. J. Eckart, D. Schneider, D. Munro, W. Stoeffl, R. Zacharias, J. J. Haslam, T. Clancy, M. Yeoman, D. Warwas, C. J. Horsfield, J.-L. Bourgade, O. Landoas, L. Disdier, G. A. Chandler, and R. J. Leeper, Rev. Sci. Instrum. **81**, 10D325 (2010).

[10] R. Hatarik, J. A. Caggiano, V. Glebov, J. McNaney, C. Stoeckl, and D. H. G. Schneider, Plasma Fusion Res. **9**, 4404104 (2014).

[11] J. H. Kunimune, J. A. Frenje, G. P. A. Berg, C. A. Trosseille, R. C. Nora, C. S. Waltz, A. S. Moore, J. D. Kilkenny, and A. J. Mackinnon, Rev. Sci. Instrum. **92**, 033514 (2021).

[12] C. Christensen, "Time-dependent neutron energy diagnostic," in 57th Annual Meeting of the APS Division of Plasma Physics, 2015.

[13] H. W. Herrmann, N. Hoffman, D. C. Wilson, W. Stoeffl, L. Dauffy, Y. H. Kim, A. McEvoy, C. S. Young, J. M. Mack, C. J. Horsfield, M. Rubery, E. K. Miller, and Z. A. Ali, Rev. Sci. Instrum. **81**, 10D333 (2010).

[14] H. Brysk, Plasma Phys. **15**, 611–617 (1973).

[15] T. J. Murphy, J. L. Jimerson, R. R. Berggren, J. R. Faulkner, J. A. Oertel, and P. J. Walsh, Rev. Sci. Instrum. **72**, 850–853 (2001).

[16] B. Appelbe and N. Hoffman, personal Communication (2021).

[17] A. S. Moore, D. J. Schlossberg, M. J. Eckart, E. P. Hartouni, T. J. Hilsabeck, J. S. Jeet, S. M. Kerr, R. Nora, and J. Kilkenny, "Constraining time-dependent ion temperature in inertial confinement fusion (ICF) implosions with an intermediate distance neutron time-of-flight (nTOF) detector" (submitted).

[18] D. Schlossberg, A. Moore, J. Kallman, M. Lowry, M. Eckart, E. Hartouni, T. Hilsabeck, S. M. Kerr, and J. D. Kilkenny, "Design of a multi-detector, single line-of-sight, time-of-flight system to measure time-resolved neutron energy spectra" (submitted).

[19] H. W. Herrmann, Y. H. Kim, A. M. McEvoy, A. B. Zylstra, C. S. Young, F. E. Lopez, J. R. Griego, V. E. Fatherley, J. A. Oertel, W. Stoeffl, H. Khater, J. E. Hernandez, A. Carpenter, M. S. Rubery, C. J. Horsfield, S. Gales, A. Leatherland, T. Hilsabeck, J. D. Kilkenny, R. M. Malone, J. D. Hares, J. Milnes, W. T. Shmayda, C. Stoeckl, and S. H. Batha, Rev. Sci. Instrum. **87**, 11E732 (2016).

[20] C. Werner, Report No. LA-UR-17-29981, 2017.

[21] N. M. Hoffman, H. W. Herrmann, Y. H. Kim, H. H. Hsu, C. J. Horsfield, M. S. Rubery, E. K. Miller, E. Grafil, W. Stoeffl, J. A. Church, C. S. Young, J. M. Mack, D. C. Wilson, J. R. Langenbrunner, S. C. Evans, T. J. Sedillo, V. Y. Glebov, and T. Duffy, Phys. Plasmas **20**, 042705 (2013).

[22] K. D. Meaney, S. Kerr, G. J. Williams, H. Geppert-Kleinrath, Y. Kim, H. W. Herrmann, D. H. Kalantar, A. Mackinnon, M. Bowers, L. Pelz, D. Alessi, D. Martinez, M. Prantil, S. Herriot, M. R. Hermann, T. E. Lanier, M. Hamamoto, J. M. Di Nicola, S. Yang, W. Williams, C. Widmayer, and R. Lowe-Webb, Phys. Plasmas **28**, 033102 (2021).